Subpicosecond optoelectronic study of resistive and superconductive transmission lines

W. J. Gallagher, C.-C. Chi, I. N. Duling, III, D. Grischkowsky, N. J. Halas,[a)]
M. B. Ketchen, and A. W. Kleinsasser
IBM Thomas J. Watson Research Center, Yorktown Heights, New York 10598

(Received 11 August 1986; accepted for publication 9 December 1986)

We have studed the propagation of subpicosecond electrical pulses on coplanar resistive and superconductive Nb transmission lines. Pulses with 0.9 ps full width at half-maximum were generated and detected by shorting fast photoconductive switches with 80 fs laser pulses. Dramatic improvements in propagation characteristics were achieved when the Nb was superconductive. We observed the strong dispersion and attenuation predicted to occur for frequency components near the superconducting energy gap frequency.

In a recent letter, Ketchen *et al.*[1] reported on the generation, propagation, and detection of subpicosecond electrical pulses on coplanar transmission lines. They were able to generate pulses with measured 1.1 ps (and inferred true 0.6 ps) full width at half-maximum (FWHM) which broadened to 2.6 ps after propagating 8 mm on a low resistance (10 Ω/mm for each line) coplanar aluminum transmission line. In this letter we report on the use of these subpicosecond electrical pulse techniques at variable temperatures (2–300 K) to study transmission lines of vastly varying resistivities, ranging from superconductive to highly lossy. In doing so we have made the fastest optoelectronic sampling measurements on a superconductor and have observed for the first time the predicted sharp onset of attenuation and strong dispersion near the superconducting pair-breaking frequency. In addition, measurements above and below the transition temperature show the dramatic improvement in pulse propagation afforded by superconductive transmission lines. Our optoelectronic sampling technique has proven to be well suited to operation inside a Dewar since all fast electrical signals (0–1 THz) are confined to the sample and only slow signals (0–2 kHz) must leave the Dewar. The technique has distinct advantages in this regard when compared to Josephson sampling techniques[2] which require high-speed electrical inputs to the cryogenic sample. Our use of fast photoconductive switches has allowed the generation and detection of pulses, in contrast to fast rise time steps used in other cryogenic optical sampling measurements.[3]

The transmission line geometries we studied consisted of two equal width (1–5 μm wide) parallel metal lines with separations equal to twice the metal linewidths (see Fig. 1). The lines were made of Nb and fabricated on commercial silicon-on-sapphire substrates (500 nm thick silicon). Lift-off patterning was used for defining 80-nm-thick Nb lines, and plasma etching was used to pattern 150- and 300-nm-thick Nb lines. Subsequent to the Nb deposition and patterning the samples received two blanket oxygen implants of 10^{15} cm^{-2} at 100 and 200 keV. The implant dosage and energy were chosen to heavily damage the Si substrate layer and thereby give the photoexcited carriers a subpicosecond lifetime for the ultrafast operation of the excitation and probe switches. The implant also slightly degraded the superconducting transition temperature of the Nb lines. In the worst case, the 80-nm-thick line had its transition temperature lowered 0.2 to 8.9 K and had a room temperature to 10 K resistivity ratio of 3 and a resistivity at 10 K of ~2 μΩ cm.

After being diced into chips, the transmission line samples were mounted on an insert in a variable temperature Dewar with an optical access window. Cold He vapor provided cooling for the sample, while temperature regulation was achieved by a feedback controlled resistive heater. The Dewar was positioned on an optical bench and 4 cm focal length lenses were used to focus two beams of 80 fs optical pulses from a dispersion compensated, colliding pulse, mode-locked ring dye laser onto the sample generation and detection points.

Electrical pulses were generated when the laser pulses momentarily shorted the photoconductive substrate in the gap region between the two charged lines of the transmission line structure. A fast photoconductive switch that connected the transmission line to an electrical probe sampled the propagating pulses produced at the movable generation point ("sliding contact"). The photoconductive switch at the sampling point was driven by a time delayed probe beam from the same laser that generated the initial electrical pulse. The electrical field of the propagating pulse was sampled by a phase sensitive measurement of the ac current induced in the sampling arm at the frequency at which either the generating or probing laser beam was chopped. By varying the time delay of the probe beam relative to the exciting beam, the time development of the electrical field as it passed the

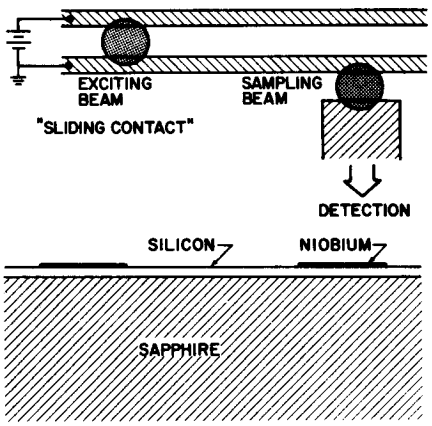

FIG. 1. Top and cross-sectional view of the transmission line geometry.

[a)] Present address: Dept. of Physics and Astronomy, Vanderbilt University, Nashville, TN 37235.

 0003-6951/87/060350-03$01.00

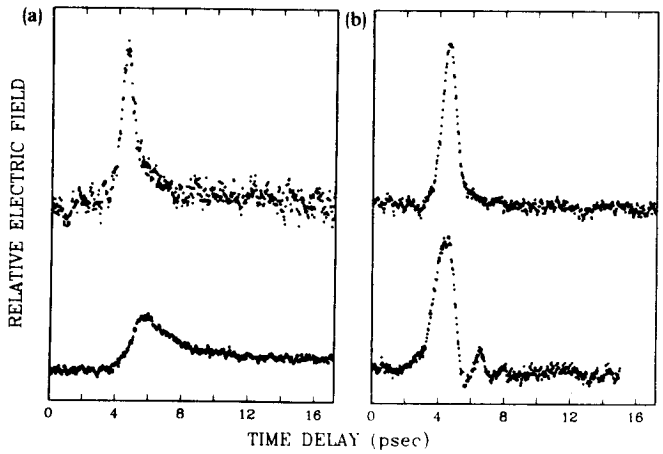

FIG. 2. (a) Pulse shapes after propagating distances of 0.5 (top) and 3 mm (bottom) on a coplanar transmission line composed of 20 Ω/mm Nb lines at 10 K. (b) Pulses after propagating the same distances on the line in the superconducting state at 2.6 K.

sampling point was mapped out. By changing the separation between the sliding contact generation point and the fixed sampling point we could study the evolution of the shape of the electrical pulse as it propagated varying distances.

Figure 2 shows the measured electric field amplitude of pulses propagated distances of 0.5 and 3 mm at temperatures of 10 and 2.6 K on the two-line coplanar transmission line. The 300-nm-thick, 5-μm-wide Nb lines comprising the transmission line had resistances of 20 Ω/mm at 10 K and a superconducting transition temperature of ~9.4 K. The top trace in Fig. 2(a) shows a pulse at 10 K after propagating 0.5 mm. It has a FWHM of 0.9 ps and shows the beginning of a tail developing on its falling edge. By the time the pulse has propagated 3 mm [lower trace in Fig. 2(a)], the pulse energy has degraded to 40% of its initial value and the pulse consists of an initial spike with a 2.3-ps FWHM superimposed on a steplike structure with a height that is 1/3 of the amplitude of the spike. This appearance of a long tail is a characteristic of propagation on lossy lines[4] (as we will discuss later), but the resistance that would be needed to explain the size of the step is about an order of magnitude larger than the dc resistance of this line. For comparison, we note that this pulse is rather severely degraded compared to the relatively good propagation characteristics of pulses on roughly comparable resistivity Al transmission lines at room temperature. Reference 1 reported that similar pulses propagated on a 10-Ω/mm aluminum line broadened to only 2.6 ps after propagating 8 mm.

Figure 2(b) shows the pulses after propagating 0.5 and 3 mm on the same Nb line when it is well into the superconducting state at 2.6 K. After the pulse has propagated 0.5 mm (top trace) on the superconducting line, its FWHM is 1.0 ps, 10% greater than it was for the normal metal state, but there is only a slight tail on the trailing edge. After propagating 3 mm (lower trace) the pulse energy degraded by only 5% and its FWHM broadened to 1.4 ps, but more significantly there is clear ringing on the trailing edge. The ringing is due to the strong dispersion at frequencies approaching the superconducting energy gap frequency of Nb at 0.7 THz and is the first observation of this phenomenon which was predicted by the superconducting transmission line calculations of Kautz[5] based on the Mattis–Bardeen[6] theory for the complex conductivity of superconductors.

Further insight into how superconductivity influences pulse propagation on lines that are highly lossy in the normal state can be gleaned by looking at Fig. 3 where we plot the electric field of a pulse after propagating 0.5 mm on a transmission line composed of two 70-nm-thick, 1.2-μm-wide Nb lines (with $T_c = 8.9$ K) at temperatures of 2.6, 6, and 10 K. The resistance at 10 K of each line in this case was ~450 Ω/mm. There is no evidence of an initial spike on the propagation characteristic in the normal state, which instead appears as a step with a very long tail. The pulses are well preserved on the superconducting lines. The measurement at 2.6 K shows ringing qualitatively similar, but of somewhat smaller relative amplitude than that in Fig. 2(b). The period of the ringing is ~23% shorter in the 2.6 K data than in the 6 K data. If for fixed distance the change in the frequency of the ringing scaled directly with the gap frequency at which strong dispersion occurs, we would have expected a ~15% decrease in the period of the ringing.

Examining the amplitude spectra of pulses propagated on the superconducting transmission line gives insight into the frequency-dependent absorption near the superconduct-

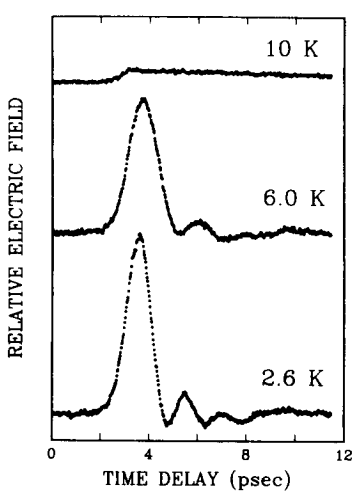

FIG. 3. Pulses after propagating 0.5 mm on a coplanar transmission line composed of 450 Ω/mm Nb lines at 10 K (top trace), 6K (middle trace), and 2.6 K (bottom trace).

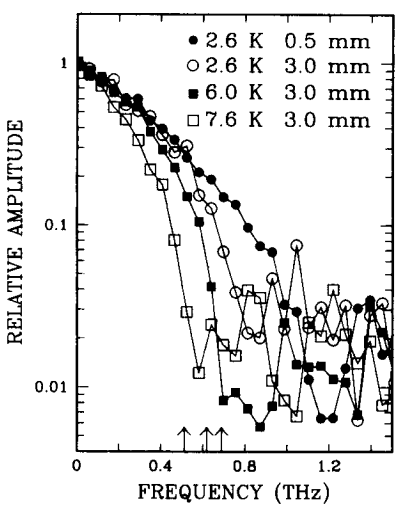

FIG. 4. Amplitude spectra of pulses propagated 3 mm on the 20 Ω/mm Nb line when superconducting at temperatures of 2.6, 6.0, and 7.6 K compared to the amplitude spectrum of the "initial" pulse (i.e., after 0.5 mm of propagation at 2.6 K). The arrows indicate the calculated pair-breaking frequencies at the three temperatures.

ing gap frequency. Figure 4 displays the amplitude spectra of data in Fig. 2(b) for the pulses propagated 0.5 and 3 mm at 2.6 K along with additional data for pulses propagated 3 mm at 6.0 and 7.5 K. With increasing temperature there is a clear decrease in the frequency at which the power is rapidly absorbed into the noise level. The increases in absorption fall very near the estimated values of the pair-breaking frequencies at 2.6, 6.0, and 7.5 K indicated by the arrows in the plot. With increasing temperature there is also an increase in absorption below the pair-breaking frequency due to energy being absorbed by the increasing density of thermally excited quasiparticles. The absorption below the pair-breaking frequency can also be seen to be increasing with frequency. The onset of strong attenuation at the gap frequency and increase in absorption below the gap with increasing temperature and frequency are both in qualitative agreement with the theoretical expectations.[5,6]

The propagation in the normal state is much worse than is expected for propagation on lossy lines characterized by the measured dc resistances. Pulses on lossy lines characterized by (frequency independent) resistances per unit length R, capacitances per unit length C, and inductances per unit length L are exponentially attenuated with a time constant $2L/R$ and have a diffusivelike tail that develops as the main pulse is attenuated. The origin of the two parts of the propagated pulse is easily understood by examining the terms in the lossy line equation

$$\frac{\partial^2 V}{\partial x^2} = LC\frac{\partial^2 V}{\partial t^2} + RC\frac{\partial V}{\partial t}. \quad (1)$$

For $R=0$ this is the ordinary wave equation. For $R>0$ there is an additional diffusive term. The crossover from wavelike behavior to diffusive behavior occurs for frequencies $f < R/2\pi L$. For our most resistive line (the 450 Ω/mm line of Fig. 3), the crossover is at $f \sim 0.09$ THz. Only 10% of the area of our pulses, estimated to have 0.6 ps FWHM (and approximated as Gaussian shaped), is below this frequency. Thus according to Eq. (1) the pulses should mainly propagate as waves and have only small diffusive tails. In contrast, after traveling only 0.5 mm on the 450 Ω/mm line in the normal state at 10 K, the pulse shape shows only a long steplike characteristic. The step rise time of ~0.65 ps is comparable to that of the launched pulse, but the tail is very long. Further measurements on a longer time scale showed that the amplitude of the tail was still 13% of the initial step height 90 ps after the initial rise. Another highly lossy line showed similar propagation characteristics. On the 80-nm-thick, 5-μm-wide Nb lines at room temperature with resistances of 500 Ω/mm, we likewise observed only the step and diffusivelike tail on pulses after they had propagated 0.5 mm.

The frequency dependence of the losses due to the skin effect could account for the observed pulse degradation on the very lossy lines. At 1 Thz the skin depth of the 450 Ω/mm line (~4 μΩ cm) is 100 nm. Current crowding would thus result in an increase of the line resistance near 1 Thz, and an increase of the crossover frequency.[7] In this case, a substantial fraction of the pulse area is in the regime where diffusive propagation dominates. Frequency-dependent losses must also be the source of the observed broadening of propagated pulses on lower resistance normal state Al and Nb lines. [No pulse broadening is expected from Eq. (1) unless some of the transmission line parameters are frequency dependent.] However, the skin effect alone cannot account for the substantially greater distortion of pulses propagating on 20 Ω/mm normal state Nb lines than that of pulses propagating on 10 Ω/mm Al lines.

It is interesting to note that the resistances per unit length of the resistive lines studied in Figs. 2 and 3 span the range of the resistances of metal interconnects in present and future very large scale integrated circuitry. Present minimum feature sizes on integrated circuits are ~1 μm and the ultimate dimensions are believed to be near 0.25 μm.[8] Near room temperature, the resistivity of good metallic films (e.g., Al) is 1–2 μΩ cm, that of typical silicides is >10 μΩ cm, and that of polysilicon is >1000 μΩ cm. A 1-μΩ cm conductor with a 1×1 μm cross section has a resistance per unit length of 10 Ω/mm while at 0.25×0.25 μm it would have 160 Ω/mm. It is clear that picosecond pulses on micron sized polysilicon lines will have difficulties propagating any but the shortest of distances (as is well known). Our normal state Nb data suggest that submicron silicide lines will also have trouble maintaining pulse integrity over millimeter distances. For lines with ~0.25 μm cross sections, possibly even the best conductors at room temperature will show the same problems over millimeter distances.

In conclusion, we have demonstrated subpicosecond electrical sampling capability at cryogenic temperatures and used it to study the propagation of subpicosecond electrical pulses on resistive and on superconductive transmission lines. On Nb lines with resistivities on the order of those expected for ~0.25-μm-diam wire, we observed degradation of subpicosecond pulses to diffusivelike pulse with long tails in less than 0.5 mm of propagation. On the same lines well into the superconductive state, we observed good pulse propagation, with significant absorption only above the pair-breaking frequency, but with some ringing associated with strong dispersion near the pair-breaking frequency.

We acknowledge the capable assistance of C. Jessen, R. L. Sandstrom, and M. Smyth for sample preparation and E. Shapiro for pointing out Ref. 4. This research was partially supported by the U.S. Office of Naval Research.

[1]M. B. Ketchen, D. Grischkowsky, T. C. Chen, C.-C. Chi, I. N. Duling, III, N. J. Halas, J.-M. Halbout, J. A. Kash, and G. P. Li, Appl. Phys. Lett. **48**, 751 (1986).

[2]P. Wolfe, B. J. Van Zeghbroeck, and U. Deutsch, IEEE Trans. Magn. **MAG-21**, 226 (1985).

[3]D. R. Dykaar, T. Y. Hsiang, and G. A. Mourou, in *Picosecond Electronics and Optoelectronics*, edited by G. A. Mourou, D. M. Bloom, and C.-H. Lee (Springer, Berlin, Heidelberg, and Tokyo, 1985), p. 249; D. R. Dykaar, R. Sobolewski, T. Y. Hsiang, G. A. Mourou, M. A. Hollis, B. J. Clifton, K. B. Nichols, C. O. Bozler, and R. A. Murphy, Topical Meeting on Ultrafast Phenomena, June 1986, Snowmass, Colorado.

[4]O. Heaviside, Electrician **19**, 295 (1887), reprinted in O. Heaviside, *Electrical Papers* (Chelsea, New York, 1970), Vol. 2, pp. 137–141; E. Hallen, *Electromagnetic Theory* (Wiley, New York, 1962), pp. 409–414.

[5]R. L. Kautz, J. Appl. Phys. **49**, 308 (1978).

[6]D. C. Mattis and J. Bardeen, Phys. Rev. **111**, 412 (1958).

[7]The current concentration also lowers the inductance, cf. R. E. Matick, *Transmission Lines for Digital and Communication Networks* (McGraw-Hill, New York, 1969), pp. 310–354. For our coplanar transmission line geometry, the inductance change is much less significant than the resistance change.

[8]P. M. Solomon, Proc. IEEE **70**, 489 (1982).